Genetic ablation of acid ceramidase in Krabbe disease confirms the psychosine hypothesis and identifies a new therapeutic target

Yedda Li[a], Yue Xu[b], Bruno A. Benitez[a], Murtaza S. Nagree[c], Joshua T. Dearborn[a], Xuntian Jiang[a], Miguel A. Guzman[d], Josh C. Woloszynek[b], Alex Giaramita[b], Bryan K. Yip[b], Joseph Elsbernd[b], Michael C. Babcock[b], Melanie Lo[b], Stephen C. Fowler[e], David F. Wozniak[f], Carole A. Vogler[d], Jeffrey A. Medin[c,g], Brett E. Crawford[b], and Mark S. Sands[a,h,1]

[a]Department of Medicine, Washington University School of Medicine, St. Louis, MO 63110; [b]Department of Research, BioMarin Pharmaceutical Inc., Novato, CA 94949; [c]Department of Medical Biophysics, University of Toronto, Toronto, ON M5S, Canada; [d]Department of Pathology, St. Louis University School of Medicine, St. Louis, MO 63104; [e]Department of Pharmacology and Toxicology, University of Kansas, Lawrence, KS 66045; [f]Department of Psychiatry, Washington University School of Medicine, St. Louis, MO 63110; [g]Pediatrics and Biochemistry, Medical College of Wisconsin, Milwaukee, WI 53226; and [h]Department of Genetics, Washington University School of Medicine, St. Louis, MO 63110

Edited by William S. Sly, Saint Louis University School of Medicine, St. Louis, MO, and approved August 16, 2019 (received for review July 15, 2019)

Infantile globoid cell leukodystrophy (GLD, Krabbe disease) is a fatal demyelinating disorder caused by a deficiency in the lysosomal enzyme galactosylceramidase (GALC). GALC deficiency leads to the accumulation of the cytotoxic glycolipid, galactosylsphingosine (psychosine). Complementary evidence suggested that psychosine is synthesized via an anabolic pathway. Here, we show instead that psychosine is generated catabolically through the deacylation of galactosylceramide by acid ceramidase (ACDase). This reaction uncouples GALC deficiency from psychosine accumulation, allowing us to test the long-standing "psychosine hypothesis." We demonstrate that genetic loss of ACDase activity (Farber disease) in the GALC-deficient mouse model of human GLD (twitcher) eliminates psychosine accumulation and cures GLD. These data suggest that ACDase could be a target for substrate reduction therapy (SRT) in Krabbe patients. We show that pharmacological inhibition of ACDase activity with carmofur significantly decreases psychosine accumulation in cells from a Krabbe patient and prolongs the life span of the twitcher (Twi) mouse. Previous SRT experiments in the Twi mouse utilized L-cycloserine, which inhibits an enzyme several steps upstream of psychosine synthesis, thus altering the balance of other important lipids. Drugs that directly inhibit ACDase may have a more acceptable safety profile due to their mechanistic proximity to psychosine biogenesis. In total, these data clarify our understanding of psychosine synthesis, confirm the long-held psychosine hypothesis, and provide the impetus to discover safe and effective inhibitors of ACDase to treat Krabbe disease.

Krabbe disease | acid ceramidase | twitcher mouse | galactosylceramidase | psychosine

Infantile globoid cell leukodystrophy (GLD, Krabbe disease) is an inherited disorder first described in 1916 that is characterized by failure to thrive, limb stiffness, seizures, developmental regression, and death by 2–4 y of age (1–3). The disease is caused by a deficiency of the lysosomal enzyme galactosylceramidase (GALC), which is responsible for degrading galactosylceramide, and the cytotoxic glycolipid, galactosylsphingosine (psychosine) (4). In 1972, Miyatake and Suzuki proposed the "psychosine hypothesis," which states that psychosine accumulation is responsible for the clinical signs associated with Krabbe disease (5). With respect to the source of psychosine, complementary evidence suggested that psychosine was synthesized through the anabolic addition of galactose to sphingosine (6, 7). Cleland and Kennedy (1960) showed that labeled galactose was incorporated into psychosine in vitro using a crude microsomal fraction from rodent brain homogenates (6). In 1973, Lin and Radin were unable to demonstrate the existence of a catabolic pathway leading to the production of psychosine, thus indirectly supporting the existence of an anabolic mechanism (7). Our data show that psychosine is generated catabolically through the deacylation of galactosylceramide by acid ceramidase (ACDase). This effectively dissociates GALC deficiency from psychosine accumulation, allowing us to test the long-standing psychosine hypothesis. We demonstrate that genetic loss of ACDase activity [Farber disease (FD) (8)] in the twitcher (Twi) (9) model, a GALC-deficient mouse that accurately models Krabbe disease, eliminates psychosine accumulation and cures GLD. We show that pharmacological inhibition of ACDase activity with carmofur, an anticancer drug that also inhibits ACD activity (10), significantly decreases psychosine accumulation and prolongs the life span of the twitcher mouse. Previous substrate reduction therapy experiments in the twitcher mouse utilized L-cycloserine, which inhibits an enzyme several steps upstream of psychosine synthesis (11, 12). Drugs that directly inhibit ACDase may have a more acceptable safety profile due to their mechanistic proximity to psychosine biogenesis. In total, these data correctly identify the mechanism of psychosine synthesis, clarify the confounding observation of no galactosylceramide accumulation in Krabbe disease, confirm the long-held

Significance

This study identifies the source of the toxic glycolipid, galactosylsphingosine (psychosine), which accumulates in the inherited demyelinating disorder, Krabbe disease. It was suggested that psychosine was produced anabolically by the addition of galactose to sphingosine. We show here instead that psychosine is derived from the catabolic deacylation of galactosylceramide by the lysosomal enzyme acid ceramidase. These findings allow us to test and confirm the ~45-y-old "psychosine hypothesis," which states that psychosine causes the pathological and clinical signs of Krabbe disease. Finally, these data suggest that acid ceramidase could be a substrate reduction target for treating Krabbe disease. We show that pharmacological inhibition of acid ceramidase significantly increases the life span of the twitcher mouse, an authentic murine model of Krabbe disease.

Author contributions: Y.L., Y.X., J.C.W., B.E.C., and M.S.S. designed research; Y.L., B.A.B., M.S.N., J.T.D., X.J., M.A.G., A.G., B.K.Y., J.E., M.C.B., and M.L. performed research; Y.L., Y.X., S.C.F., and J.A.M. contributed new reagents/analytic tools; Y.L., D.F.W., C.A.V., and M.S.S. analyzed data; and Y.L. and M.S.S. wrote the paper.

Conflict of interest statement: Y.X., J.C.W., A.G., B.K.Y., J.E., M.C.B., M.L., and B.E.C. are employees of BioMarin Pharmaceutical. The remaining authors declare no conflict of interest.

This article is a PNAS Direct Submission.

[1]To whom correspondence may be addressed. Email: mssands@wustl.edu.

This article contains supporting information online at www.pnas.org/lookup/suppl/doi:10.1073/pnas.1912108116/-/DCSupplemental.

First published September 16, 2019.

psychosine hypothesis, and identify acid ceramidase as a potential therapeutic target for Krabbe disease and possibly other sphingolipidoses.

Results and Discussion

The well-established function of ACDase is to catalyze the degradation of lysosomal ceramides into sphingosine and fatty acids (Fig. 1*A*). The ceramide that is degraded by ACDase originates from several sources, including de novo synthesis of ceramides, or from degradation products of numerous ceramide derivatives, including glycosphingolipids and sphingomyelins. Recently, ACDase was also shown to catalyze the deacylation of glucosylceramide to glucosylsphingosine (13, 14). Glucosylceramide and galactosylceramide are stereoisomers. Enzyme–substrate interactions are typically stereospecific; nevertheless, we hypothesized that ACDase can deacylate galactosylceramide to form psychosine (catabolic reaction, Fig. 1*B*). In a pure in vitro system, we showed that recombinant ACDase deacylated an analog of galactosylceramide to psychosine (Fig. 2*A*). While ACDase can catabolize galactosylceramide, the enzyme is much less efficient at the deacylation of galactosylceramide compared to ceramide (*SI Appendix*, Fig. 1). To determine if the same reaction occurs in vivo, we created a mouse (Twi/FD) harboring homozygous mutations in both the GALC and ACDase (15) genes. Psychosine accumulates to high levels in dermal fibroblasts from Twi mice compared to wild-type (WT) or FD mice (Fig. 2*B*). In contrast, cells from Twi/FD mice do not accumulate psychosine (Fig. 2*C*). However, lentiviral-mediated reconstitution of ACDase activity in cells from Twi/FD mice results in the accumulation of high levels of psychosine (Fig. 2*C*).

To determine if the same reaction occurs in intact animals, we surveyed the brain, sciatic nerve, liver, and spleen from Twi/FD mice for psychosine accumulation. The levels of psychosine in the Twi/FD tissues were indistinguishable from those in WT and FD animals and were significantly lower than those in Twi mice both at 36 d of age (Fig. 2 *D*–*G*) and when killed (*SI Appendix*, Fig. S2*A*). Homozygous mutations in the human ACDase gene cause Farber disease, a rapidly progressing lysosomal storage disorder characterized by the widespread accumulation of ceramide (8). Elevated ceramide levels in liver and spleen, 2 severely affected organs in Farber disease, were observed in FD and Twi/FD mice but not in WT or Twi mice at 36 d (Fig. 2 *H* and *I*) or at the terminal time point (*SI Appendix*, Fig. S2*B*).

Together, the data presented here strongly suggest that psychosine is produced primarily through a catabolic mechanism (Fig. 1*B*). In the previously published in vitro experiments directly supporting the existence of an anabolic pathway (6), it is likely that the crude brain homogenates contained an enzyme (perhaps ceramide galactosyltransferase) that incorporated the labeled galactose into galactosylceramide, which was then converted to psychosine by ACDase. With respect to the prior attempts to confirm a catabolic mechanism for psychosine production (7), the authors mention in the discussion that they, in fact, detected minute levels of psychosine. Although we show compelling in vitro and in vivo data suggesting that the catabolic pathway is the primary mechanism for psychosine production, these data do not formally exclude the existence of an anabolic pathway. If an anabolic pathway exists, its contribution is minimal since there is no psychosine accumulation observed in the Twi/FD mice even at the terminal time points.

In the Twi/FD mouse, GALC deficiency is uncoupled from psychosine accumulation, allowing us to test the long-standing, yet unproven, psychosine hypothesis. The mean maximum body weight of Twi/FD mice (18.1 ± 1.8 g) was indistinguishable from that of FD mice (18.2 ± 1.9 g) and significantly greater than that of Twi mice (12.2 ± 1.9 g) (Fig. 3*A*). Both Twi/FD and FD mice had splenomegaly and thymic hypertrophy compared to WT and Twi mice (Fig. 3 *B* and *C*). Tremor is a defining characteristic of the Twi mouse (9, 16, 17) but has never been reported in the FD mice. At 36 d, the peak tremor frequencies (PTFs) observed in Twi/FD and FD mice (9.0 ± 4.0 and 8.6 ± 2.2 Hz, respectively) were not different from those of WT animals (9.1 ± 2.2 Hz) but significantly lower than those of Twi mice (17.4 ± 2.2 Hz) (Fig. 3*D*). By 63 d, Twi/FD (14.6 ± 5.9 Hz) and FD (16.6 ± 3.7 Hz) mice trended higher than WT mice (9.8 ± 2.2 Hz) in PTF but were not significantly different from each other (*SI Appendix*, Fig. S3*A*). Untreated Twi mice develop severe motor impairment (16, 17). At 36 d, Twi/FD and FD mice performed near WT

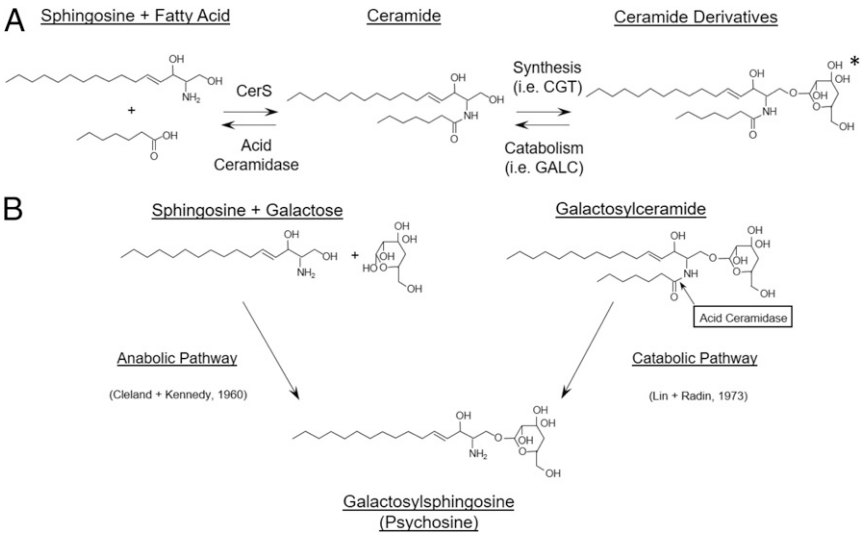

Fig. 1. Role of ACDase in ceramide degradation and psychosine synthesis. (*A*) ACDase is responsible for the lysosomal degradation of ceramides originating from various cellular sphingolipid sources. The ceramide derivative shown is galactosylceramide (the asterisk [*] indicates that galactose can be substituted by sulfated galactose, glucose, sialic acid, oligosaccharides, phosphocholine, or phosphate residues; synthesized; and catabolized by other enzymes). CerS and CGT are abbreviations for ceramide synthase and ceramide galactosyltransferase, respectively. (*B*) Psychosine can potentially be synthesized either through the anabolic dehydration of sphingosine and galactose (*Left*) or through the catabolic deacylation of galactosylceramide by acid ceramidase (*Right*). Two studies have directly (5) or indirectly (6) supported the anabolic pathway.

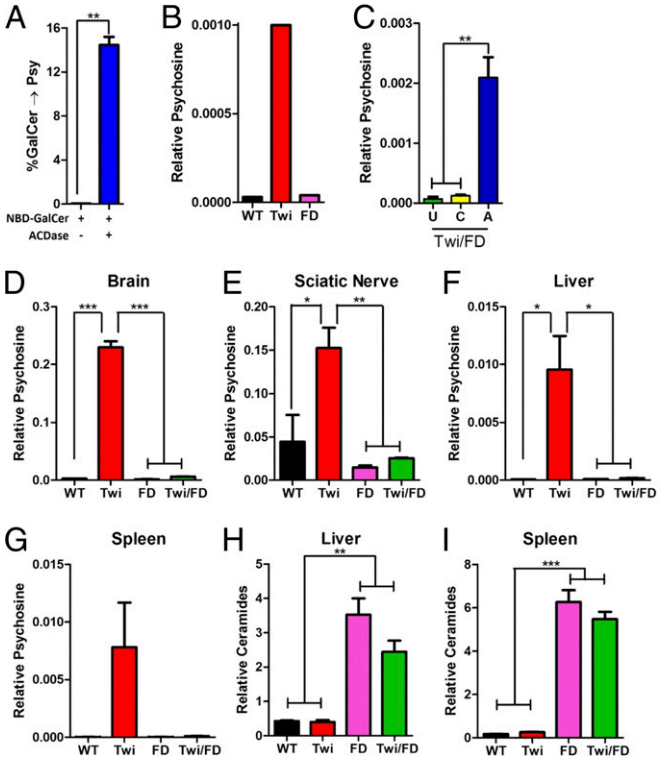

Fig. 2. Acid ceramidase catalyzes the formation of psychosine in vitro and in vivo. (*A*) Recombinant ACDase catalyzes the deacylation of galactosylceramide (GalCer) to psychosine in vitro. (*B*) Twi fibroblasts accumulate psychosine compared to WT or FD fibroblasts. (*C*) Reconstitution of ACDase activity following lentiviral transduction of Twi/FD fibroblasts (A) dramatically increases psychosine accumulation compared to untransduced (U) cells or cells transduced with a control virus (C). Thirty-six day-old Twi mice accumulate high levels of psychosine in the brain (*D*), sciatic nerve (*E*), liver (*F*), and spleen (*G*) compared to WT, FD, and Twi/FD mice. Ceramide is elevated in the liver (*H*) and spleen (*I*) of FD and Twi/FD mice compared to WT or Twi mice. $*P \leq 0.05$, $**P \leq 0.01$, $***P \leq 0.001$.

levels on both the rotarod (Fig. 3*E*) and wire hang (Fig. 3*F*), while Twi mice exhibited significant deficits on both tests. By 63 d, Twi/FD and FD mice have significant motor deficits but are indistinguishable from each other (*SI Appendix*, Fig. S3 *B* and *C*). The median life span of Twi/FD mice (63 d) was significantly longer than that of Twi mice (42 d) and slightly shorter than that of FD mice (74 d) (Fig. 3*G*). Galactosylceramides were significantly elevated in the sciatic nerve of Twi/FD mice compared to Twitcher mice (Fig. 3*H*). This indicates that ACDase cleaves galactosylceramide regardless of fatty acyl chain length (Fig. 3*H*). The slight but significant shortening of life span in Twi/FD mice may be due to the unique accumulation of galactosylceramide. This is a consequence of concurrent GALC and ACDase deficiency and likely results in toxic effects. Regardless, these data are consistent with both GALC and ACDase participating in the in vivo metabolism of galactosylceramide. This may explain the confounding observation that human Krabbe patients and Twi mice do not accumulate high levels of galactosylceramide in the central nervous system (18, 19).

Mice with a Farber-like disease are characterized by significantly increased circulating monocytes and neutrophils and decreased T cells compared to normal controls (20). The hematological abnormalities in 60-d-old Twi/FD mice were similar to those observed in age-matched FD mice with larger circulating monocyte ($Ly6G^{-}Ly6C^{hi}$) and neutrophil ($Ly6G^{+}Ly6C^{+}$) populations and significantly smaller T cell ($CD3^{+}$) populations compared to WT mice (*SI Appendix*, Fig. 3*D*).

Histologically, Twi/FD mice showed little or no signs of Twi pathology. At 36 d of age, Luxol fast blue (LFB) and periodic acid–Schiff (PAS) staining of Twi cerebellum showed abnormal myelin morphology, numerous "globoid cells," and widespread microglial/macrophage activation (CD68+) (Fig. 4*A*). There was a significant increase in activated macrophages/microglia in the cerebellum of twitcher mice compared to WT and Twi/FD mice (Fig. 4*B*). Farber disease mice had fewer globoid cells in the white matter tracts and decreased microglial activation compared to Twi mice. Histologically, Twi/FD mice were indistinguishable from FD mice. At the terminal time point, mild microglial activation was observed in Twi/FD mice that was indistinguishable from FD mice (*SI Appendix*, Fig. S3*E*).

At 36 d of age, there were inflammatory infiltrates and edema in Twi sciatic nerves compared to WT sciatic nerves (Fig. 4*A*). There was a significant decrease in the axon density in the twitcher mice compared to WT, FD, and Twi/FD mice (Fig. 4*C*). On ultrastructural examination, the twitcher mice appear to have thinner myelin sheaths, axons of smaller diameter, endoneural edema, collagen deposition, and infiltrating macrophages compared to wild-type animals (Fig. 4*A*). Sciatic nerves from FD mice and Twi/FD mice were indistinguishable from each other and appeared similar to those of wild-type animals with intact axonal structures; few, if any, infiltrating inflammatory cells; and little or no edema (Fig. 4*A*). This same pattern was observed at a

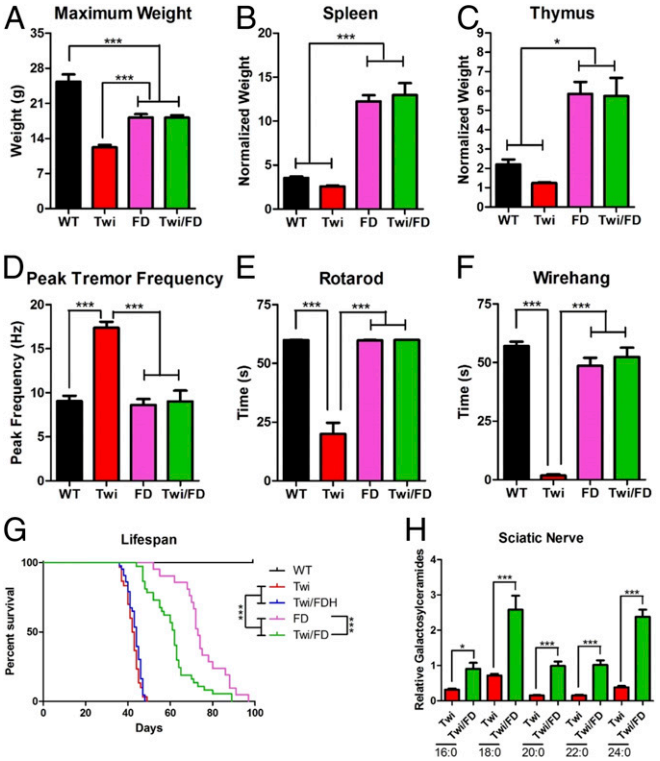

Fig. 3. Confirmation of the psychosine hypothesis. (*A*) The mean maximum body weight and normalized spleen (*B*) and thymus (*C*) weights in Twi/FD mice are not significantly different from those of FD mice but are significantly greater than those of Twi mice. (*D*) At 36 d, a prominent tremor is observed in Twi mice but not in WT, Twi/FD, or FD mice. Twi mice have significant motor deficits as measured by the rotarod (*E*) and wire-hang (*F*) tests compared to WT, FD, and Twi/FD mice at 36 d. (*G*) Median life span of Twi/FD mice (63 d) is significantly longer than that of Twi (42 d) and Twi/FDH (42 d) mice and slightly shorter than that of FD mice (74 d). (*H*) All of the galactosylceramide species assayed (16:0, 18:0, 20:0, 22:0, and 24:0) are significantly elevated in the sciatic nerve of 36-d-old Twi/FD mice compared to twitcher mice. $*P \leq 0.05$, $***P \leq 0.001$.

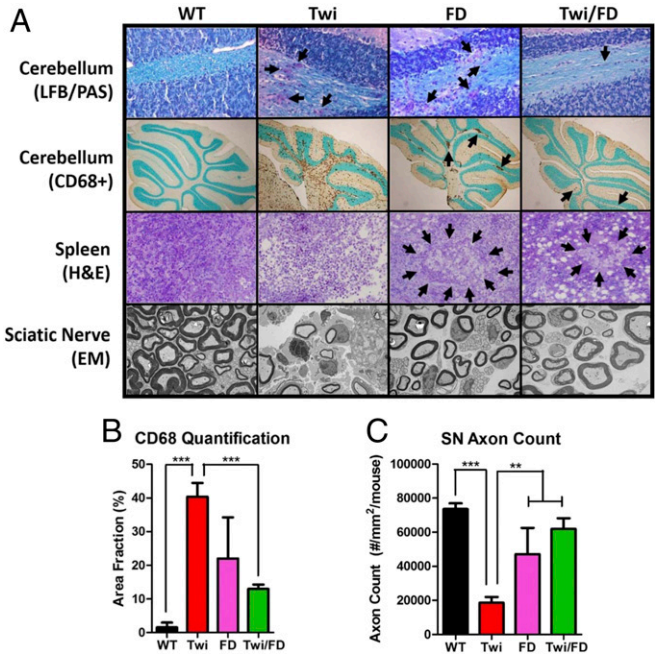

Fig. 4. Histological correction of the twitcher phenotype. (*A*) Luxol fast blue/periodic acid–Schiff (LFB/PAS) staining of cerebellum shows disorganized myelin and increased numbers of globoid cells (arrows) in the 36-d-old Twi mouse compared to WT, FD, and Twi/FD mice. Twi mice have diffuse and widespread cerebellar CD68+ microgliosis that is most prominent in the white matter tract compared to WT mice. Microgliosis is less apparent and focal (arrows) in FD and Twi/FD mice. Hematoxylin and eosin (H&E) staining of the spleens of Twi mice shows a general disruption of the splenic architecture with no evidence of intracellular storage material. FD and Twi/FD mice have abundant splenic intracellular storage material (arrows). Ultrastructural analysis of the sciatic nerves of Twi mice shows endoneural edema, infiltrating macrophages, and collagen with thinner myelin sheaths compared to WT mice. The FD and Twi/FD sciatic nerves are virtually indistinguishable from normal and are identical to each other. (*B*) There is a significant decrease in CD68-positive cells in WT, FD, and Twi/FD mice compared to Twi mice. (*C*) Quantification of axon counts in 36-d-old mice shows significantly fewer axons in Twi mice compared to WT, FD, or Twi/FD mice. $^{**}P \leq 0.01$, $^{***}P \leq 0.001$.

terminal age (*SI Appendix*, Fig. S3 *E* and *F*). Spleens from Twi mice contained inflammatory infiltrates but no vacuoles (Fig. 4*A*). In contrast, spleens of age-matched FD and Twi/FDH mice contained very few inflammatory infiltrates but were heavily vacuolated.

The nearly complete elimination of the biochemical, behavioral, and histological phenotypes of the Twi mouse by genetic ablation of ACDase activity confirms the psychosine hypothesis. Although GALC deficiency may have unanticipated clinical effects later in life, those effects appear to progress more slowly than the acute toxicity mediated by psychosine.

Because the hypomorphic $Asah1^{P361R/P361R}$ mutation eliminates psychosine accumulation as well as the clinical features of Krabbe disease, we hypothesized that pharmacologic inhibition of ACDase activity could improve the Twi phenotype. Carmofur is a 5-fluorouracil-releasing chemotherapeutic agent (21) that also directly inhibits ACDase activity (10). Carmofur significantly inhibits ACDase-mediated psychosine formation in vitro (Fig. 5*A*). Psychosine levels are significantly decreased when GALC-deficient fibroblasts from a patient with Krabbe disease are treated with carmofur (Fig. 5*B*). The carmofur-treated Krabbe cells had significantly elevated levels of ceramide (Fig. 5*C*). Twice-daily intraperitoneal (i.p.) injections of carmofur in $GALC^{-/-}$, $Asah1^{+/-}$ (Twitcher/Farber Disease Heterozygote [Twi/FDH]) mice significantly reduced ACDase activity in the liver (Fig. 5*D*). Carmofur-treated Twi and Twi/FDH mice had significantly decreased psychosine levels in the brain compared to vehicle-treated animals (Fig. 5*E*). Interestingly, this regimen did not increase ceramide levels (Fig. 5*F*). Finally, carmofur administration significantly increased the median life span of Twi/FDH mice (Fig. 5*G*).

Experimental substrate reduction therapy (SRT) for Krabbe disease has been limited to L-cycloserine (12, 17), which reduces psychosine accumulation by inhibiting serine palmitoyltransferase, an enzyme several steps upstream of psychosine synthesis. As such, L-cycloserine disrupts several other critical sphingolipid pathways (11). The data presented here strongly suggest that ACDase might be a better SRT target for Krabbe disease due to its proximity to psychosine biogenesis. However, safer inhibitors will likely be required before inhibition of ACDase activity can be exploited clinically. Although carmofur was able to increase the life span of Twi/FDH mice, significant drug-associated toxicity (22) may have contributed to the decreased life span observed in some treated Twi mice and limited the efficacy in Twi/FDH mice. Finally, the increased life span observed in Twi/FDH ($Asah1^{+/-}$) but not Twi ($Asah1^{+/+}$) mice suggests that i.p. injection

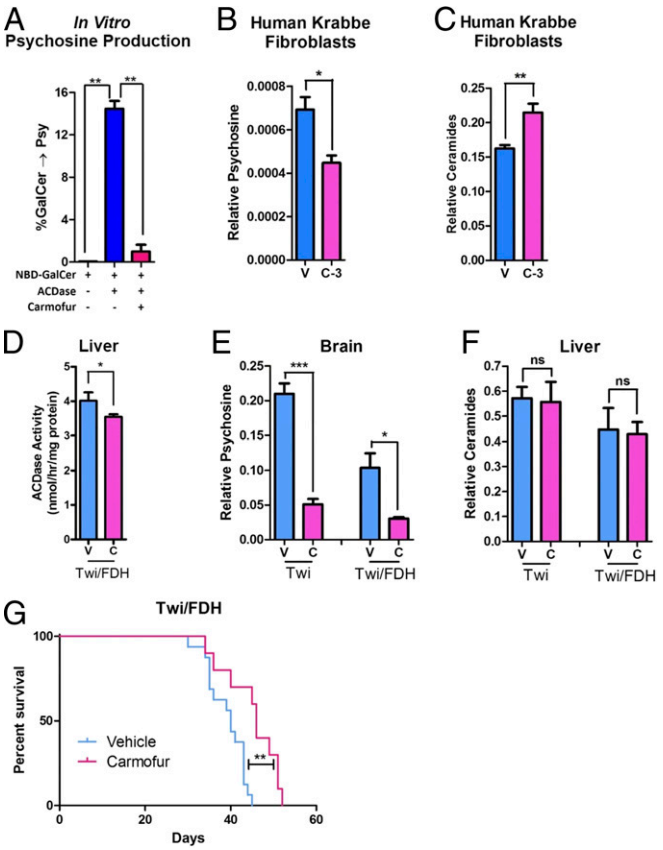

Fig. 5. Acid ceramidase as a target for substrate reduction therapy. (*A*) Carmofur efficiently inhibits acid ceramidase activity against galactosylceramide in vitro. (*B*) Carmofur (3 μM, C-3) decreases psychosine accumulation in human fibroblasts from a Krabbe patient compared to vehicle (V). (*C*) Carmofur increases ceramide accumulation in human fibroblasts from a Krabbe patient. (*D*) Acid ceramidase activity is decreased in the liver of Twi/FDH mice treated with carmofur. (*E*) Psychosine is decreased in the livers of Twi and Twi/FDH mice following twice-daily i.p. injections of carmofur (C) at 30 mg/kg compared to vehicle (V). (*F*) Ceramides are not elevated in the brains of the same mice shown in *E*. Twice-daily i.p. injections of carmofur significantly increases the median life span of Twi/FDH mice (*G*) compared to vehicle controls. $^{*}P \leq 0.05$, $^{**}P \leq 0.01$, $^{***}P \leq 0.001$; ns, $P > 0.05$.

of carmofur is not sufficient to inhibit the full complement of ACDase activity.

Substrate reduction therapy with L-cycloserine synergizes with other therapies, such as gene therapy and bone marrow transplantation, to dramatically increase efficacy in the Twi mouse (17, 23). Substituting an ACDase inhibitor for L-cycloserine in a similar combination therapy regimen would likely greatly enhance therapeutic efficacy. Finally, although only partially effective, it is important to note that carmofur treatment did not increase ceramide accumulation in the liver. This suggests that there may be a therapeutic window where ACDase activity can be sufficiently inhibited to decrease psychosine levels without inducing significant ceramide accumulation and Farber disease–like symptoms.

Together, these results identify the major pathway (catabolic) for psychosine synthesis in vitro and in vivo: the deacylation of galactosylceramide by ACDase. These data demonstrate that both GALC and ACDase partially degrade galactosylceramide, which may account for the puzzling lack of galactosylceramide accumulation in human and murine Krabbe disease (18, 19). We have confirmed the long-standing psychosine hypothesis (at least within the life span of Twi/FD mice) by demonstrating that GALC-deficient mice do not develop Krabbe phenotypes in the absence of psychosine accumulation. We also identify ACDase as a novel SRT target, providing the impetus to discover safe and effective inhibitors for the treatment of Krabbe disease. Finally, lysosphingolipids accumulate in several sphingolipidoses and recently have been shown to be toxic to cells in culture (24). Thus, these findings will likely have implications for disorders beyond Krabbe disease.

Methods

Experimental Animals. Animals were housed at Washington University in St. Louis under the supervision of M.S.S. Heterozygous Twi ($GALC^{+/-}$) mice on a C57BL/6 background (Jackson Laboratory) were bred with heterozygous FD ($Asah1^{+/P361R}$) mice on a mixed C57BL/6 and 129Sv background (provided by J.A.M.) (15) to generate double-heterozygous ($GALC^{+/-}$, $Asah1^{+/-}$) animals. Double-heterozygous animals were crossed with each other to generate $GALC^{-/-}$, $Asah1^{-/-}$ (Twi/FD, 1/16); $GALC^{-/-}$, $Asah1^{+/-}$ (Twi/FDH, 1/8); $GALC^{+/+}$, $Asah1^{-/-}$ (FD, 1/16); $GALC^{-/-}$, $Asah1^{+/+}$ (Twi, 1/16); and $GALC^{+/+}$, $Asah1^{+/+}$ (WT, 1/16). Genotypes of all experimental mice were determined by PCR, as previously described for the Twi mouse (25) and the FD mouse (15). Mice were housed under standard conditions with ad libitum access to food and water. Mice were maintained on a 12 h/12 h light/dark cycle. All animal procedures were approved by the Institutional Animal Care and Use Committee at Washington University School of Medicine and were in accordance with the guidelines of the NIH.

Recombinant Acid Ceramidase. Human acid ceramidase constructs were prepared for production in Chinese hamster ovary (CHO) cells. A human full-length acid ceramidase complementary DNA (cDNA) was subcloned into a mammalian expression vector. The CHO cells were grown in suspension in chemically defined medium. Clones expressing the highest amount of acid ceramidase protein were isolated and expanded. The acid ceramidase protein was produced in shaker flasks with a fed-batch production. Additional feeds and glucose were provided during the 10- to 14-d culture process. Cell culture fluid was harvested, filtered, and stored at −80C until the purification process. Recombinant acid ceramidase was purified via a 2-step chromatographic procedure. The cell culture harvest was thawed, and the pH was adjusted to 7.0, followed by sterile filtration. The filtered material was loaded onto a Capto Q (GE Healthcare) column, preequilibrated with 20 mM Tris, pH 7.0, followed by linear NaCl gradient elution. Elution peak samples were loaded onto a Butyl Sepharose 4 FF (GE Healthcare) column, preequilibrated with 20 mM Tris, 1M NaCl, pH 7.0. The bound acid ceramidase protein was eluted under stepwise NaCl gradient conditions. Purified samples were concentrated using centrifugal spin concentrators and sterile filtered for storage.

Psychosine Production in Vitro. To determine whether ACDase could directly cleave galactosylceramide, 20 μmol of C12-*N*-[6-[(7-nitro-2-1,3-benzoxadiazol-4-yl)amino]hexanoyl]-D-galactosylceramide (C12-NBD-galactosylceramide) (Cayman Chemical) were incubated with 5 to 10 μg of purified acid ceramidase in a 30 μL reaction containing 15 μL of 0.2 M citrate phosphate buffer (pH 4.5), 2.25 μL of 2 M NaCl, 1.5 μL of 10 mg/mL bovine serum albumin (BSA), and 0.3 μL of 10% IGEPAL CA630. The reaction was incubated at 37 °C for 18 h without agitation and then stopped by adding 60 μL of acidified methanol. The amount of psychosine formed by the deacylase activity of the enzyme was determined by monitoring the release of NBD-fatty acid on an Acquity UPLC (excitation, 435 nm; emission, 525 nm). To compare the efficiency of ACDase substrates, 26 μmol of C12-NBD-galactosylceramides or C12-NBD-ceramides were incubated at 37 °C with 1.0 μg of enzyme for 3 h or 24 h using the above buffer conditions and detection method for monitoring the production of NBD-fatty acid.

Lentivirus Preparation. The ASAH1 (experimental lentivirus) and α-galactosidase A (AGA, control lentivirus) vectors were provided by J.A.M. Generation of the transfer plasmid, pDY-AGA, was described previously (26). pDY-ASAH1 was constructed using similar methods. Briefly, the full-length human ASAH1 cDNA was subcloned into the lentiviral transfer plasmid (pDY) to generate pDY-hASAH1. Lentiviral stocks were prepared by transient transfection of HEK293T cells using a 4-plasmid system (pCMVΔR8.91, pMD.G, pAdV, and the transfer plasmids) and concentrated by centrifugation. Concentrated viral stocks were titered using HEK293T cells, and vector copy number was determined by quantitative PCR as previously described.

Mouse and Human Fibroblast Manipulations. Primary subdermal fibroblasts from WT, FD, Twi, and Twi/FD mice were isolated from newborn animals and grown in Dulbecco's modified Eagle media (DMEM) supplemented with 15% heat-inactivated fetal bovine serum (FBS), 10 mM Hepes buffer, minimum essential media (MEM) nonessential amino acid solution, 1 mM sodium pyruvate, and 1% penicillin/streptomycin under 5% pCO_2 at 37 °C. Cells were grown to ∼50% confluence, then transduced with lentivirus-expressing acid ceramidase or α-galactosidase A (control) with a multiplicity of infection of ∼50. The serum was dropped to 1% 72 h after transduction. Fibroblasts were maintained in 1% serum level for 1 wk, after which they were harvested, pelleted, and stored at −80 °C for psychosine and ceramide measurements. Three biological replicates were performed for each condition.

Early passage (p5) primary human fibroblasts from an 8-mo-old patient with Krabbe disease were obtained from the Coriell Institute (GM04517). The donor was homozygous for a 30 kb deletion that eliminates exons 11 to 17 of the GALC gene and results in no GALC activity. The cells were grown in DMEM supplemented with 10% heat-inactivated FBS, 10 mM Hepes buffer, MEM nonessential amino acid solution, 1 mM sodium pyruvate, and 1% penicillin/streptomycin under 5% pCO_2 at 37 °C. When the cells reached ∼80% confluence, the FBS concentration was reduced to 0.5%, and 3 μM carmofur (LKT Laboratories) or vehicle (dimethyl sulfoxide [DMSO]) was added. A complete media change with fresh carmofur or vehicle was performed every 24 h for 2 wk. The cells were then harvested and analyzed by mass spectrometry for psychosine and ceramide levels. Six biological replicates were performed for each condition.

Mass Spectrometry. Galactosylsphingosine (psychosine), galactosylceramide, and ceramides were measured in the brain, liver, sciatic nerve, and spleen, essentially as previously described (27, 28). Tissue samples were homogenized in 0.04 M citric acid. Internal controls in 200 μL methanol were added to 50 μL of each sample. Galactosylsphingosine and galactosylceramide were separated from glucosylsphingosine and glucosylceramide by hydrophilic interaction liquid chromatography (HILIC) columns. Ceramides were separated by 2-dimensional column chromatography with HILIC as the first dimension and reversed phase column chromatography as the second dimension. Multiple reaction monitoring was used to detect galactosylsphingosine, ceramide, and galactosylceramide on an AB SCIEX 4000QTRAP tandem mass spectrometer (Atlantic Lab Equipment) using electrospray ionization in the positive ion mode. Data processing was conducted with Analyst 1.5.2 (Applied Biosystems). Data are reported as the peak area ratios of lipids to their internal standards. Only data for 16:0 acylated species of ceramides and galactosylceramides are shown in this paper. The relative levels of other ceramide species were similar to the 16:0 acylated species among the different genotypes, unless otherwise indicated.

Histology. Luxol fast blue and periodic acid–Schiff staining were performed essentially as described (16). Briefly, mice were deeply anesthetized and perfused with phosphate-buffered saline (PBS); then pieces of spleen, liver, and one sagittal half of the brain were harvested immediately. Tissue samples were cryoprotected in 30% sucrose after being fixed in 4% paraformaldehyde in PBS for 24 to 48 h at 4 °C. Tissues were embedded in

paraffin for LFB/PAS staining. Ten-micrometer sections were mounted on slides for analysis.

Sciatic nerves were isolated following perfusion with PBS and immersion fixed in 4% paraformaldehyde/2% glutaraldehyde in PBS. Nerves were incubated in osmium tetroxide and then serially dehydrated in ethanol. After embedding in Araldite 502 (Polysciences), 1 μm sections were prepared using an ultramicrotome and stained with toluidine blue. After mounting on slides, images were acquired using a Hitachi CCD KP-MIAN digitizing camera mounted on a Leitz Laborlux S microscope. Histomorphometric analysis was carried out using the Leco IA32 Image Analysis System as previously described (16). Briefly, the total number of axons was counted in 3 different high-power fields from each sample, corresponding to an area of 0.005 mm^2. The axon counts were then averaged and converted to axons/square millimeter. For electron microscopy (Fig. 4*A*), 70 nm thick sections were obtained and stained with uranyl acetate and lead citrate, and images were obtained on a JEOL 1400 Plus transmission electron microscope (magnification = 5,000×).

Immunohistochemistry. One sagittal half of each brain was harvested immediately following perfusion with PBS and fixed in 4% paraformaldehyde for 24 to 48 h at 4 °C, then cryoprotected in 30% sucrose. Sixteen-micrometer cryosections were blocked in normal goat serum, then incubated with primary rabbit anti-mouse glial fibrillary acidic protein (GFAP) (Immunostar) antibody or rat anti-mouse CD68 (Bio Rad), as previously described (16). The sections were then incubated with the appropriate horseradish peroxidase-conjugated secondary antibody and developed with a commercially available DAB kit (Vector Laboratories).

Life Span, Body Weight, and Behavioral Testing. Life span was recorded as the age at which an animal spontaneously died or was killed for humane reasons as defined by one or more of the following: >25% loss of maximum body weight, lethargy, and lack of response to tactile stimulation. All animals were killed by anesthetic overdose. Experimental animals were weighed at least twice a week for the duration of their lives, and the maximum weight for each animal was recorded. Organs were removed, weighed, and then normalized to body weight. Behavioral testing consisted of the rotarod and wire-hang tests, which were conducted as previously reported (16). Starting on postnatal day (PND) 21, the mice were trained on each apparatus by performing the tests 3 times on each of 3 consecutive days. Those data are not included in the final analysis. Mice were then tested once every other week on the constant-speed (3 rpm) rotarod and once every week on the wire-hang starting at PND 28. Performance was measured as the time it took the mouse to fall from either apparatus. On each test day, 3 trials were conducted for each test, and the average of the 3 trials was reported. For both tests, the maximum tested time was 60 s. There were $n = 11$ mice, $n = 17$ mice, $n = 17$ mice, and $n = 10$ mice tested for the WT, Twi, FD, and Twi/FD experimental groups, respectively.

Actometer Testing. Tremor severity was quantified using a custom-made force-plate actometer as previously described (29). Animals were acclimated for at least 30 min in the procedure room prior to tremor monitoring. Recordings from the transducers were collected at 100 samples/s. The most frequently occurring tremor frequency (Hz) in a continuously measured period of 10 min was reported for each mouse. There were $n = 13$ mice, $n = 10$ mice, $n = 10$ mice, and $n = 11$ mice tested for the WT, Twi, FD, and Twi/FD experimental groups, respectively.

Flow Cytometry. Circulating hematopoietic-derived cells from experimental and control animals were identified and quantified by fluorescence-activated cell sorting. Red blood cells were lysed, and cells were stained with 7-AAD and fluorophore-conjugated antibodies after blocking the Fc receptor. The following antibodies were used: FITC rat anti-mouse CD3 (T cells, BD Biosciences), APC rat anti-mouse CD11b (monocytes, neutrophils, eBioscience), PE-Cey7 anti-mouse Ly6G (monocytes, neutrophils, eBioscience), and eFluor-450 rat anti-mouse Ly6C (monocytes, neutrophils, eBioscience). Data were acquired on a Gallios flow cytometer (Beckman Coulter) and analyzed using FlowJo software (Tree Star).

Carmofur Administration. A stock solution of carmofur at 300 mg/kg was made in DMSO and stored at −20 °C. Stock solutions were diluted in Solutol (Sigma-Aldrich) and citrate buffer to make the 3 mg/mL working solution immediately prior to each injection. To determine the effects of carmofur treatment on life span, Twi and Twi/FDH animals were injected i.p. with carmofur (30 mg/kg) or vehicle every 12 h starting at postnatal day 10 for the remainder of their lives. To determine the effects of carmofur on ACDase activity in vivo, Twi/FDH mice received the same dosing regimen as described above and were killed at 28 d of age. The livers were harvested and analyzed for ACDase activity.

Acid Ceramidase Activity Assay. Acid ceramidase activity was measured in tissue lysates using Rbm14-12 substrate as previously reported (30). Briefly, tissue was homogenized in 0.2 M sucrose with protease inhibitor mixture (Thermo Scientific), and lysates were prepared by the freeze–thaw method. Lysates were cleared by centrifugation at 19,000 g for 10 min and stored at −80 °C. Protein concentration was determined using a bicinchoninic acid (BCA) assay (Thermo Scientific). Lysates (25 μg protein/well) were mixed with 2 nmol of Rbm14-12 (RUBAM) in sodium acetate (pH 4.5) in opaque microtiter plates and incubated for 3 h at 37 °C. The reaction was stopped with 50 μL methanol and 100 μL of 2.5 mg/mL sodium periodate in 0.1 M glycine (pH 10.6) and incubated at 37 °C for 2 h in the dark. Fluorescence was measured with excitation at 355 nm and emission at 460 nm. All assays were performed in triplicate.

Statistical Analysis. All quantitative data are reported as the mean ± 1 SEM. Statistical significance was calculated using one-way ANOVA with a Bonferroni correction for multiple comparisons. *P* values are denoted as follows: $*P \leq 0.05$; $**P \leq 0.01$; $***P \leq 0.001$; ns denotes not significant ($P > 0.05$).

ACKNOWLEDGMENTS. This work was supported by grants from BioMarin Pharmaceutical and NIH NS100779 (to M.S.S.); NIH HL007088 (to Y.L.); NIH HD087011 and the Taylor Institute (to D.F.W.); The Inaugural MACC (Midwest Athletes Against Childhood Cancer) Fund Endowed Chair (to J.A.M.); and NIH HD02528 (to S.C.F.). Marie Roberts and Kevin O'Dell (Washington University) provided excellent technical assistance on mouse husbandry, injections, and behavioral assays. Doug Covey created the biochemical structures shown in Fig. 1*B*. Mika Aoyagi-Scharber, Terri Christianson, Vishal Agrawal, John E. Pak, and Megi Rexhepaj (BioMarin Pharmaceutical) provided intellectual and technical assistance for the creation of the cell lines and preparation and purification of recombinant acid ceramidase. The measurement of galactosylsphingosine (psychosine), galactosylceramide, and ceramides was performed in the Washington University Metabolomics Facility (NIH P30 DK020579 and P30 DK056341).

1. K. Krabbe, A new familial, infantile form of diffuse brain-sclerosis. *Brain* **39**, 74–114 (1916).
2. B. Hagberg, P. Sourander, L. Svennerholm, Diagnosis of Krabbe's infantile leucodystrophy. *J. Neurol. Neurosurg. Psychiatry* **26**, 195–198 (1963).
3. D. A. Wenger, M. A. Rafi, P. Luzi, Krabbe disease: One hundred years from the bedside to the bench to the bedside. *J. Neurosci. Res.* **94**, 982–989 (2016).
4. K. Suzuki, Y. Suzuki, Globoid cell leucodystrophy (Krabbe's disease): Deficiency of galactocerebroside β-galactosidase. *Proc. Natl. Acad. Sci. U.S.A.* **66**, 302–309 (1970).
5. T. Miyatake, K. Suzuki, Globoid cell leukodystrophy: Additional deficiency of psychosine galactosidase. *Biochem. Biophys. Res. Commun.* **48**, 539–543 (1972).
6. W. W. Cleland, E. P. Kennedy, The enzymatic synthesis of psychosine. *J. Biol. Chem.* **235**, 45–51 (1960).
7. Y. N. Lin, N. S. Radin, Alternate pathways of cerebroside catabolism. *Lipids* **8**, 732–736 (1973).
8. T. Levade, K. Sandhoff, H. Schulze, J. A. Medin, *Acid Ceramidase Deficiency: Farber Lipogranulomatosis. Online Metabolic and Molecular Bases of Inherited Disease*, D. Valle *et al*., Eds. (McGraw-Hill, New York, NY, 2009).
9. L. W. Duchen, E. M. Eicher, J. M. Jacobs, F. Scaravilli, F. Teixeira, Hereditary leucodystrophy in the mouse: The new mutant twitcher. *Brain* **103**, 695–710 (1980).
10. N. Realini *et al*., Discovery of highly potent acid ceramidase inhibitors with in vitro tumor chemosensitizing activity. *Sci. Rep.* **3**, 1035 (2013).
11. K. S. Sundaram, M. Lev, Inhibition of sphingolipid synthesis by cycloserine in vitro and in vivo. *J. Neurochem.* **42**, 577–581 (1984).
12. S. M. LeVine, T. V. Pedchenko, I. G. Bronshteyn, D. M. Pinson, L-cycloserine slows the clinical and pathological course in mice with globoid cell leukodystrophy (twitcher mice). *J. Neurosci. Res.* **60**, 231–236 (2000).
13. Y. Yamaguchi, N. Sasagasako, I. Goto, T. Kobayashi, The synthetic pathway for glucosylsphingosine in cultured fibroblasts. *J. Biochem.* **116**, 704–710 (1994).
14. M. J. Ferraz *et al*., Lysosomal glycosphingolipid catabolism by acid ceramidase: Formation of glycosphingoid bases during deficiency of glycosidases. *FEBS Lett.* **590**, 716–725 (2016).
15. A. M. Alayoubi *et al*., Systemic ceramide accumulation leads to severe and varied pathological consequences. *EMBO Mol. Med.* **5**, 827–842 (2013).
16. A. S. Reddy *et al*., Bone marrow transplantation augments the effect of brain- and spinal-cord-directed AAV 2/5 gene therapy by altering inflammation in the murine model of GLD. *J. Neurosci.* **31**, 9945–9957 (2011).
17. J. A. Hawkins-Salsbury *et al*., Mechanism-based combination treatment dramatically increases therapeutic efficacy in murine globoid cell leukodystrophy. *J. Neurosci.* **35**, 6495–6505 (2015).
18. Y. Eto, K. Suzuki, K. Suzuki, Globoid cell leukodystrophy (Krabbe's disease): Isolation of myelin with normal glycolipid composition. *J. Lipid Res.* **11**, 473–479 (1970).
19. L. Svennerholm, M.-T. Vanier, J.-E. Månsson, Krabbe disease: A galactosylsphingosine (psychosine) lipidosis. *J. Lipid Res.* **21**, 53–64 (1980).

20. S. Dworski *et al*., Markedly perturbed hematopoiesis in acid ceramidase deficient mice. *Haematologica* **100**, e162–e165 (2015).
21. M. Watanabe *et al*., Randomized trial of the efficacy of adjuvant chemotherapy for colon cancer with combination therapy incorporating the oral pyrimidine 1-hexylcarbamoyl-5-fluorouracil. *Langenbecks Arch. Surg.* **391**, 330–337 (2006).
22. S. Kuzuhara *et al*., Subacute leucoencephalopathy induced by carmofur, a 5-fluorouracil derivative. *J. Neurol.* **234**, 365–370 (1987).
23. S. Biswas, S. M. LeVine, Substrate-reduction therapy enhances the benefits of bone marrow transplantation in young mice with globoid cell leukodystrophy. *Pediatr. Res.* **51**, 40–47 (2002).
24. C. J. Folts, N. Scott-Hewitt, C. Pröschel, M. Mayer-Pröschel, M. Noble, Lysosomal re-acidification prevents lysosphingolipid-induced lysosomal impairment and cellular toxicity. *PLoS Biol.* **14**, e1002583 (2016).
25. N. Sakai *et al*., Molecular cloning and expression of cDNA for murine galactocerebrosidase and mutation analysis of the twitcher mouse, a model of Krabbe's disease. *J. Neurochem.* **66**, 1118–1124 (1996).
26. J. Huang *et al*., Lentivector iterations and pre-clinical scale-up/toxicity testing: Targeting mobilized CD34+ cells for correction of Fabry disease. *Mol. Ther. Methods Clin. Dev.* **5**, 241–258 (2017).
27. J. Sikora *et al*., Acid ceramidase deficiency in mice results in a broad range of central nervous system abnormalities. *Am. J. Pathol.* **187**, 864–883 (2017).
28. R. Sidhu *et al*., A HILIC-MS/MS method for simultaneous quantification of the lysosomal disease markers galactosylsphingosine and glucosylsphingosine in mouse serum. *Biomed. Chromatogr.* **32**, e4235 (2018).
29. S. C. Fowler *et al*., A force-plate actometer for quantitating rodent behaviors: Illustrative data on locomotion, rotation, spatial patterning, stereotypies, and tremor. *J. Neurosci. Methods* **107**, 107–124 (2001).
30. C. Bedia, L. Camacho, J. L. Abad, G. Fabriàs, T. Levade, A simple fluorogenic method for determination of acid ceramidase activity and diagnosis of Farber disease. *J. Lipid Res.* **51**, 3542–3547 (2010).